View metadata, citation and similar papers at core.ac.uk

brought to you by CORE

provided by HKU Scholars Hub

Title	Design, synthesis and biological characterization of novel inhibitors of CD38
Author(s)	Dong, M; Si, YQ; Sun, SY; Pu, XP; Yang, ZJ; Zhang, LR; Zhang, LH; Leung, FP; Lam, CMC; Kwong, AKY; Yue, J; Zhou, Y; Kriksunov, IA; Hao, Q; Cheung Lee, H
Citation	Organic And Biomolecular Chemistry, 2011, v. 9 n. 9, p. 3246-3257
Issued Date	2011
URL	http://hdl.handle.net/10722/137500
Rights	Creative Commons: Attribution 3.0 Hong Kong License

Organic & Biomolecular Chemistry

Dynamic Article Links

Cite this: DOI: 10.1039/c0ob00768d

www.rsc.org/obc

PAPER

Design, synthesis and biological characterization of novel inhibitors of CD38†

Min Dong,[a] Yuan-Qi Si,[a] Shuang-Yong Sun,[a] Xiao-Ping Pu,[a] Zhen-Jun Yang,[a] Liang-Ren Zhang,[a] Li-He Zhang,*[a] Fung Ping Leung,[b] Connie Mo Ching. Lam,[b] Anna Ka Yee Kwong,[b] Jianbo Yue,[b] Yeyun Zhou,[c] Irina A. Kriksunov,[c] Quan Hao[b] and Hon Cheung Lee*[b]

Received 23rd September 2010, Accepted 17th February 2011
DOI: 10.1039/c0ob00768d

Human CD38 is a novel multi-functional protein that acts not only as an antigen for B-lymphocyte activation, but also an enzyme catalyzing the synthesis of a Ca^{2+} messenger molecule, cyclic ADP-ribose, from NAD^+. It is well established that this novel Ca^{2+} signaling enzyme is responsible for regulating a wide range of physiological functions. Based on the crystal structure of the CD38/NAD^+ complex, we synthesized a series of simplified *N*-substituted nicotinamide derivatives (**Compound 1–14**). A number of these compounds exhibited moderate inhibition of the NAD^+ utilizing activity of CD38, with **Compound 4** showing the ~~higher~~ potency. The crystal structure of CD38/**Compound 4** complex and computer simulation of **Compound 7** docking to CD38 show a significant role of the nicotinamide moiety and the distal aromatic group of the compounds for substrate recognition by the active site of CD38. Biologically, we showed that both **Compounds 4** and **7** effectively relaxed the agonist-induced contraction of muscle preparations ~~form~~ rats and guinea pigs. This study is a rational design of inhibitors for CD38 that exhibit important physiological effects, and can serve as a model for future drug development.

Introduction

CD38 is a *trans*-membrane enzyme, originally identified as a lymphocyte differentiation antigen.[1] It is now known to be ubiquitously expressed in virtually all mammalian tissues examined.[2] As a multi-functional protein and a member of the ADP-ribosyl cyclase family, CD38 catalyzes the synthesis of cyclic ADP-ribose (cADPR) from NAD^+, a cyclic nucleotide messenger mediating Ca^{2+} release from intracellular stores in a wide range of biological systems from plant to human.[3] Remarkably, CD38 can also hydrolyze the product, cADPR, and the substrate, NAD^+, to produce ADP-ribose.[4] That CD38 is ~~the~~ naturally occurring enzyme responsible for the synthesis of cADPR has been shown by ablation of the CD38 gene in mice, which results in large reduction in endogenous cADPR in many tissues.[5,6] The CD38 knockout mice exhibit a variety of defects, establishing the importance of CD38 as a regulator of diverse physiological functions,[5,6] which include immune cell differentiation,[7] α-adrenoceptor signaling in aorta,[8] hormonal signaling in pancreatic acinar cells,[9] migration of dendritic cell precursors,[10] bone resorption,[11] insulin secretion,[5,12] and social behavior changes.[13] Clinically, CD38 expression is a negative prognostic marker for chronic lymphocytic leukemia.[14,15] Moreover, CD38 is responsible for synthesizing yet another ubiquitous Ca^{2+} messenger, nicotinic acid adenine dinucleotide phosphate (NAADP), from NADP and nicotinic acid *via* a base-exchange reaction.[16,17] It should now be a generally accepted fact that CD38 is expressed both in intracellular organelles, such as the nucleus, ER, *etc.*, as well as on the surface of some cells, particular the blood cells. It is ~~our belief~~ that internal CD38 may be more relevant for cell signaling.

That CD38 plays key roles in physiology provides an important impetus for this study to design and synthesize inhibitors of CD38. Inhibitors of the enzymatic activities of CD38 have been described, but none of them have been shown to have physiological effects. Slama *et al.* synthesized a non-hydrolyzable analog of NAD^+, dinucleotide carbanicotinamide adenine dinucleotide (carba-NAD^+), as a competitive inhibitor of the NAD^+ glycohydrolase activity of CD38 with ~~the~~ IC_{50} about 100 μM.[18,19] Inhibitors that form covalent intermediates with the catalytic residues of CD38 have also been described. These inhibitors are mainly NAD^+ derivatives with modifications at the nicotinamide ribonucleoside. For example, a series of fluoro-substituted NAD^+ derivatives has been produced.[20,21] The fluoro substitution at the 2′-position of the nicotinamide sugar moiety promotes the formation of a stable covalent bond between the ribose and Glu226, the catalytic

[a]*State Key Laboratory of Natural and Biomimetic Drugs, School of Pharmaceutical Sciences, Peking University, Beijing 100191, China. E-mail: zdszlh@bjmu.edu.cn; Fax: +86-10-82802724; Tel: +86-10-82801700*

[b]*Department of Physiology, University of Hong Kong, Hong Kong, China. E-mail: leehc@hku.hk; Fax: +852-2817-1334; Tel: +852-2819-9163*

[c]*MacCHESS, Cornell High Energy Synchrotron Source, Cornell University, Ithaca, NY 14853, USA*

† Electronic supplementary information (ESI) available. See DOI: 10.1039/c0ob00768d

muscle preparations from rat and guinea pig

residue of CD38, during catalysis. The covalent intermediate has been captured by X-ray crystallography.[22] Based on the structure of ara-F NAD, Schramm and coworkers reported that ara-F NMN and several β-nicotinamide 2′-deoxyribosides are also potent inhibitors of CD38 with ~~the~~ K_i values in the nanomolar range.[21,23]

These inhibitors, being derivatives of NAD^+, are charged molecules with limited permeability to cells and tissues and none has been reported to exhibit biological effects. It is the purpose of this study to develop membrane-permeant CD38 inhibitors as tools for physiological investigations and as potential drug candidates as well. Based on the crystal structure of the CD38/NAD^+ complex that we reported previously,[24] we synthesized a series of simplified *N*-substituted nicotinamide derivatives (Fig. 2, **1–14**) and showed that some of them, including **Compounds 4** and **7**, are good inhibitors of the enzymatic activities of CD38. X-Ray crystallography shows that **Compound 4** binds inside the catalytic cavity of CD38 and reveals important details of the interacting residues at the active site. Moreover, when applied to ~~guinea pigs tracheal muscle strips~~, both **Compounds 4** and **7** exhibit ~~a~~ potent relaxing ~~effect~~ on the agonist-induced tension.

effects

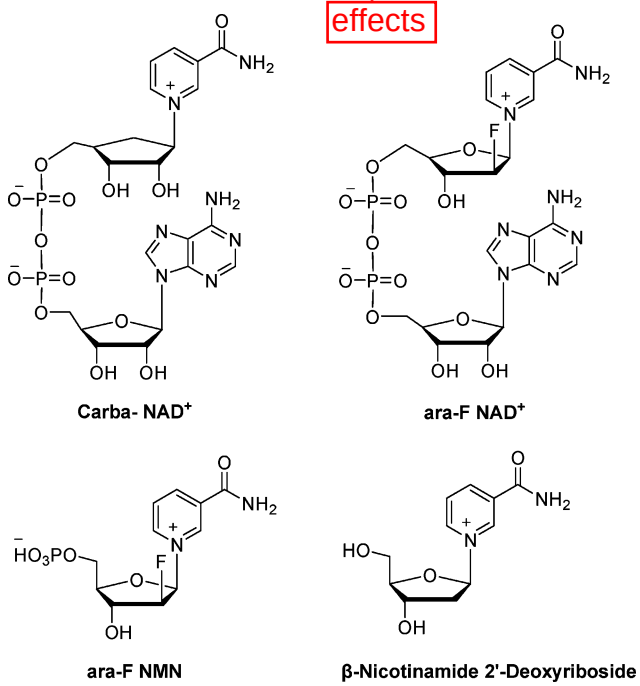

Q4 **Fig. 1** Inhibitors of **CD38**.

Results and discussion

Chemistry

The crystal structure of the CD38/NAD^+ complex shows that the nicotinamide group of the bound NAD^+ enters the catalytic cavity first and interacts with residues Glu146 and Asp155 at the active site through two hydrogen bonds to its amide. The interaction is further enhanced by the parallel π interactions between its pyridine ring and the Trp189 indole ring.[24b] It is reasoned that derivatives consisting of either one nicotinamide (**Compounds 1–7**) or bis-nicotinamide moiety (**Compounds 8–11**) may have sufficient affinity for the catalytic cavity of CD38 to serve as inhibitors. In addition, a series of derivatives was designed with aromatic ether strands replacing the adenosine-pyrophosphate moiety of the natural substrate, NAD^+, so as to improve the membrane permeability of the compounds. Finally, in **Compounds 13** and **14**, 4-amino-nicotinamide and 6-quinoline carboxylic amide replaced and mimicked the nicotinamide ring, respectively.

Compounds 1 and **2** were synthesized as depicted in Scheme 1.[25] Starting from 1,3-dioxolane and acetyl chloride, the chloromethoxyl ethyl acetate was obtained in 62% yield, which was stirred with nicotinamide for 10 h in DMF at room temperature[26] to form **Compound 1** with high yield (80%). **Compound 2** was produced by the condensation of [2-(benzyloxy)ethoxy]methyl chloride[27] and nicotinamide in DMF in 60% yield.

Compounds 3–7 were synthesized by a similar strategy. Substituted phenols or 8-hydroxyl-quinoline were condensed with chloroethanol in a 10% NaOH solution.[28] The corresponding alcohols were chloromethylated by paraformaldehyde and dry HCl in DCE. The chloromethylation products were used directly to react with nicotinamide to produce **Compounds 3–7** in good yields (Scheme 2).

8-OH-quinoline was coupled with 1,4-butenediol by Mitsunobu reaction in 70% yield. The chloromethylation product was obtained as described before and then condensed with nicotinamide to give **Compound 12** in 55.8% for two steps. (Scheme 3)

The syntheses of the bis-nicotinamide **Compounds 8–11** were completed by the condensation of the bis-chloromethylation products with two equivalents of nicotinamide, in high yields. 1,2-Bis- chloromethoxyethane, 1,4-bis-chloromethoxybutane, 1,4-bis-chloromethoxycrotonylene and 1,6-bis-chloromethoxyhexane[29] were prepared from the corresponding dihydroxyl compounds by chloromethylation reaction, as described before. (Scheme 4)

4-Phenoxyphenol was coupled with chloroethanol and then chloromethylated. The product was condensed with quinoline-6-carboxylic amide or 4-amino nicotinamide,[30] respectively, in DMF for 12 h at room temperature to produce **Compounds 13** (63%) and **14** (43%) in two steps (Scheme 5).

Biological activities

Inhibition of the activity of NADase. The newly synthesized **Compounds 1–14** were tested for their inhibitory properties against the NAD-glycohydrolase activity of the recombinant CD38, which was measured using a fluorimetric and highly sensitive coupled enzyme assay as previously described.[31] As shown in Table 1, compounds **3,4,5,7,12,13** and **14** exhibit weak inhibitory activities. Structurally, compounds with an aromatic group at the distal end from the nicotinamide are more effective in inhibiting

Q5 **Table 1** NADase inhibitory activity of **1–14**

Inhibitor	**1**	**2**	**3**	**4**	**5**	**6**	**7**
IC_{50}/mM[a]	NM	NM	11.41	3.42	5.65	NM	10.00
Inhibitor	**8**	**9**	**10**	**11**	**12**	**13**	**14**
IC_{50}/mM[a]	NM	NM	NM	NM	3.45	2.12	4.80

[a] NM = not measurable.

This journal is © The Royal Society of Chemistry 2011

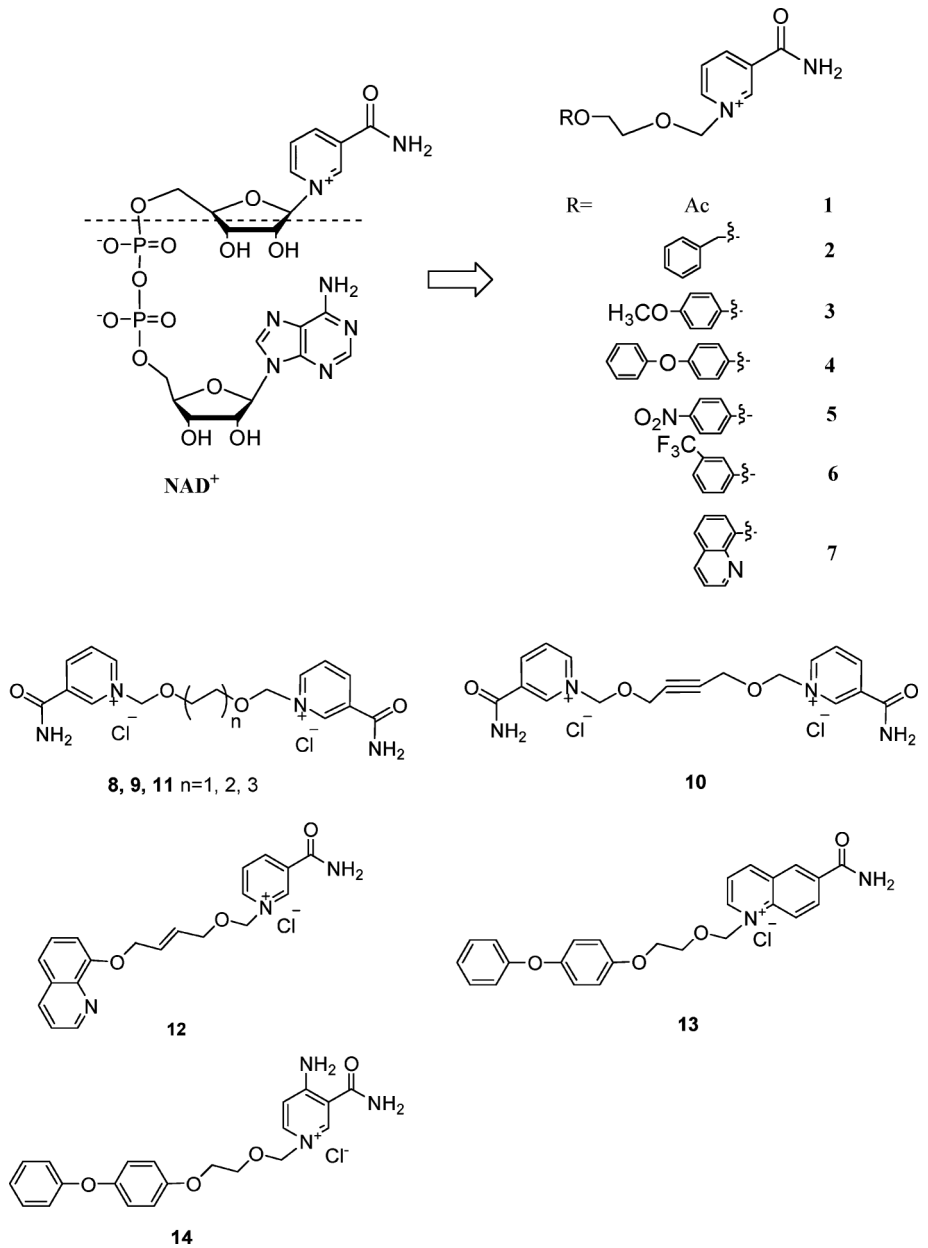

Q3

Fig. 2 NAD^+ and N-aromatic ether substituted nicotinamides.

CD38. This is likely to be due to the enhanced hydrophobic interactions with the active site. **Compound 6** contains a strong electron withdrawing *m*-CF_3-phenol group that should interfere with hydrophobic interaction, and it indeed showed no affinity for CD38. The positively charged bis-nicotinamide moiety in **Compounds 8–11** likewise ~~should~~ prohibit hydrophobic interaction and the compounds were, ~~likewise,~~ ineffective in inhibiting CD38. Interestingly, the longer aliphatic chain in **Compound 12**, as compared to **Compound 7**, improves this compound's interaction with CD38. Comparing **Compounds 13** and **4**, replacing the nicotinamide with a quinoline ring, improved the affinity slightly. On the other hand, the additional amino group on the nicotinamide ring in **Compound 14** offered no improvement as compared to **Compound 4**.

Physiological effects on muscle preparations from rat and guinea pigs

It has previously been shown that CD38 gene ablation attenuates the contraction induced by α-adrenoceptor stimulation in mouse aorta, indicating that the contraction is mediated by the CD38/cADPR-pathway.[8] We therefore tested the effect of compound **4** on the phenylephrine-induced contraction in rat aortic ring preparations with intact endothelium. As shown in Fig. 3A, compound **4** produced concentration-dependent relaxation with a half-maximal effect (pD2) at about 36 μM. The effect is specific because the structurally similar but inactive compound **9** produced no such vascular relaxing effect. Nicotinamide, a commonly used inhibitor of CD38, can effectively attenuate

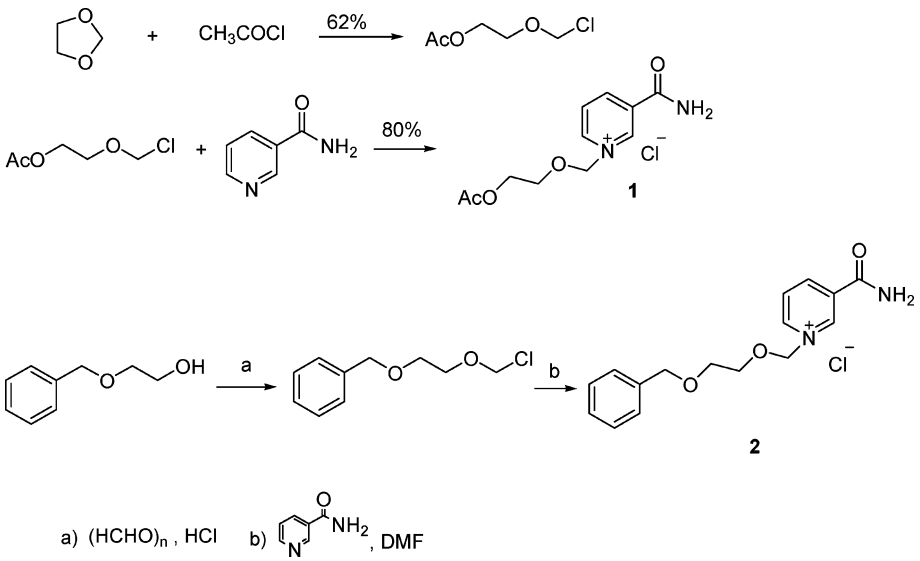

Scheme 1 Synthesis of analogues **1** and **2**.

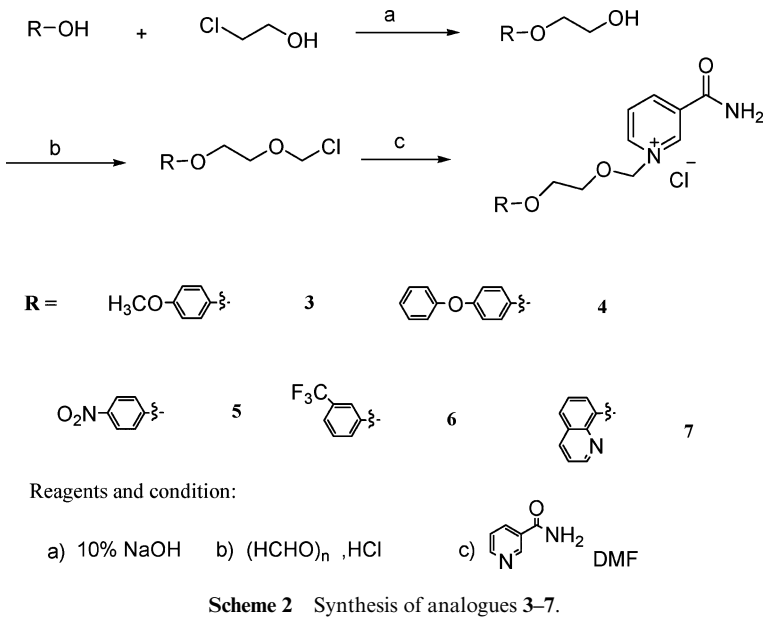

Scheme 2 Synthesis of analogues **3–7**.

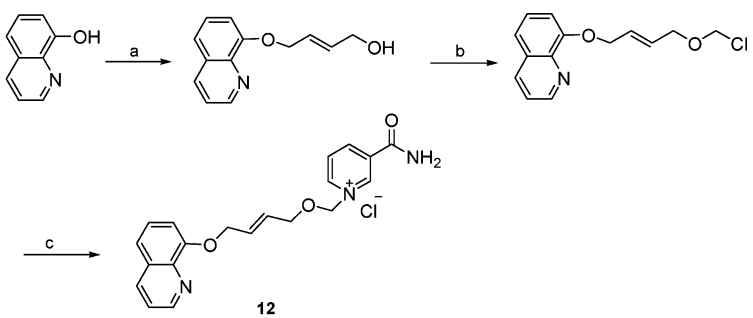

Scheme 3 Synthesis of analogues **12**.

 This journal is © The Royal Society of Chemistry 2011

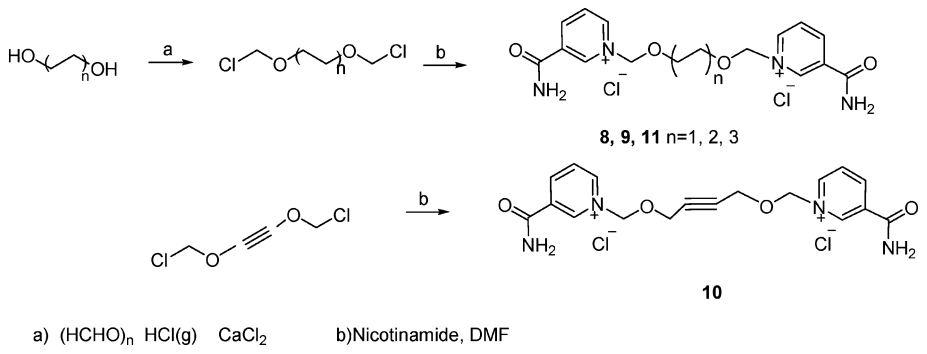

Scheme 4 Synthesis of **8–11**.

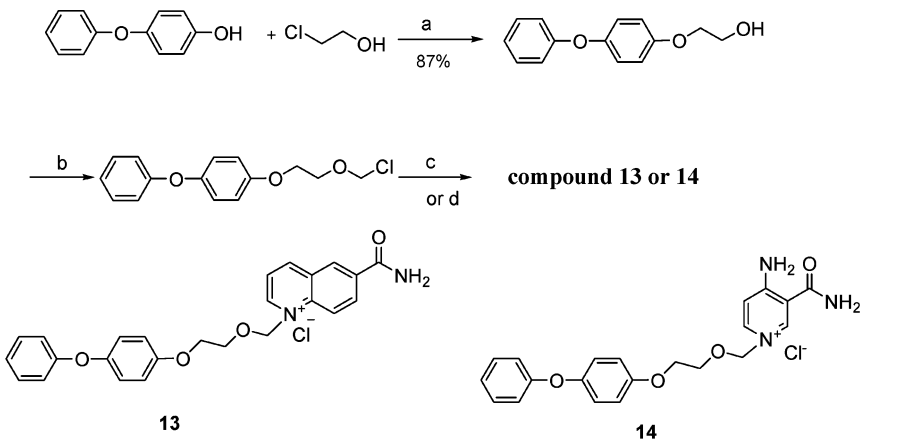

Scheme 5 Synthesis of analogues **13** and **14**.

agonist-induced contraction.[32] Fig. 3B shows that it can induce vascular relaxation in a manner similar to compound **4**. The half-maximal effect was at about 1 mM.

We have previously shown that **Compound 7**, the less potent of the series with an IC_{50} of 10 mM for the inhibition of the NADase, significantly inhibited the acetylcholine (Ach)-induced Ca^{2+} increase in PC12 cells. That the effect of Ach is mediated by CD38 is shown by RNAi knockdown of the enzyme, which completely abrogates the ACh-induced production of cADPR.[33] Airway smooth muscle contraction requires elevation of intracellular Ca^{2+}. Studies indicate that the CD38/cADPR/RyR-Ca^{2+} signaling pathway plays a vital role in the regulation of Ca^{2+} homeostasis in the airway smooth muscle cells.[34] Here we use the newly synthesized inhibitors to illustrate the role of CD38 in mediating the Ach-induced contraction in airway smooth muscle. The isolated tracheal strips of guinea pigs and rats were first contracted by treatment with Ach. The ability of the CD38 inhibitors to relax the contraction was then used as a model for the antispasmodic effects of the compounds. As shown in Fig. 3, both **Compounds 4** and **7**, ~~the most active and lower active compounds in our series,~~ were effective in relaxing the Ach-induced contraction in a dose-dependent manner. Similar results were also observed in the isolated tracheal strips of rat (data not shown). These results are consistent with the known fact that CD38 is important in mediating the Ach-induced contraction in airway smooth muscle.[34] But more importantly, the results illustrate the usefulness of these new inhibitors for investigating the physiological roles of CD38 in cells and tissues.

Although, these inhibitors show only moderate activity *in vitro*, they are much more effective *in vivo*. This is likely because of the hydrophobicity of the compounds, allowing them to easily penetrate the cell membrane and accumulate inside cells and tissues. We have calculated the AlogP using Pipeline Pilot V7.5 and the results indicate clearly that compounds **4** and **7** are more lipophilic than compound **9**.†

As is shown below, the ~~compounds bind~~ inside the catalytic pocket of CD38. It is ~~also~~ possible that the ~~structure as w~~ the residues constituting the active ~~site of rats~~ and guinea ~~pigs~~ CD38 may be somewhat different from those of the human CD38, which was used in all the *in vitro* assays. Currently, the structures of neither rat nor guinea ~~pigs~~ CD38 have been solved.

Compound 4 binds

sites of rat

pig

pig

Structural study of the binding of Compounds 4 and 7 to CD38

To understand the interactions between CD38 and these inhibitors, we prepared the complex of **Compound 4** with CD38 and analyzed it using X-ray crystallography. Pre-formed crystals of the catalytic domain of CD38 were soaked in the cryoprotectant

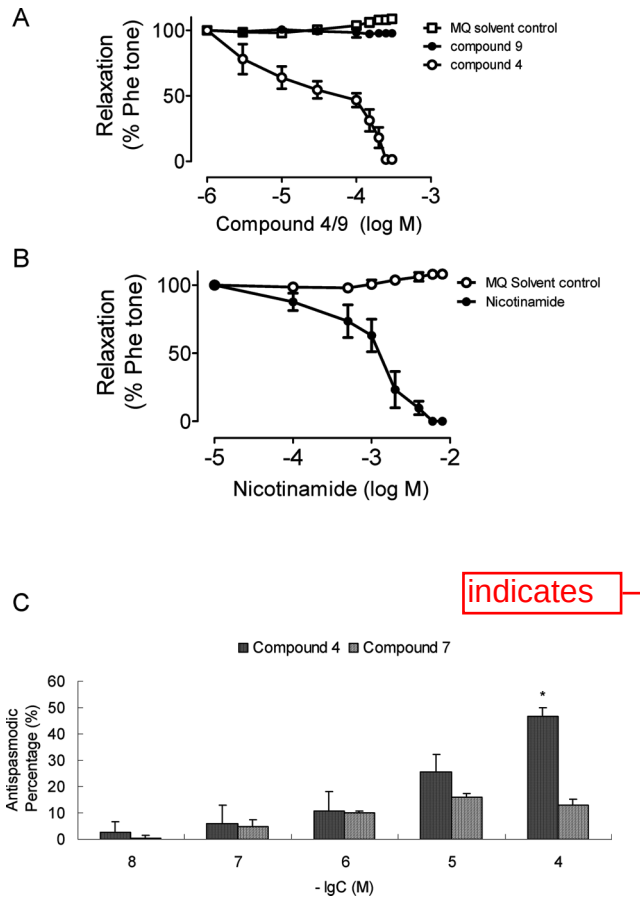

Fig. 3 Biological effects of compounds **4**, **7** and **9** on agonist-induced muscle contraction. A. Concentration-response curves for solvent (MQ water) control, compound **4** (active) and compound **9** (inactive), on the phenylephrine-induced vascular contraction in isolated rat aortic ring preparations. B. Nicotinamide, a commonly used inhibitor of CD38, induced similar vascular relaxation. Results are means ± SEM. using tissues from three to five rats in each group. C. The relaxing effects of **Compounds 4** and **7** on the acetylcholine-induced contraction in isolated tracheal strips of guinea pigs. Data represent the mean ± SEM (n = 7). $*P < 0.05$, statistically significant as compared with Krebs–Henseleit solution group.

buffer containing the compound to obtain the complex. We were able to obtain only the complex with **Compound 4** (the ESI shows the statistics of data collection and structure refinement of the complex†). Fig. 4A shows that **Compound 4** binds inside the catalytic pocket of human CD38. Superimposed in the figure is the bound NAD previously determined by us.[24] As can be seen, the nicotinamide groups of both **Compound 4** and NAD bind at the same position. They also interact identically with the same residues, forming hydrogen bonds with Glu146 and Asp155, as well as hydrophobically stack with Trp189 (Fig. 4A). The structural results indicate that the inhibitory effect of **Compound 4** is likely to be due to its specific binding to the active site. The *N*-substituted biphenyl ether group in **Compound 4** distal to the nicotinamide ring, on the other hand, binds quite differently than the ribose and phosphate groups of NAD, interacting instead mainly with Trp176 through hydrophobic stacking (Fig. 4A).

Molecular dynamics simulation allows us to model the interaction of **Compound 7** with CD38, even though we were unable to obtain the crystal complex. The stimulation was carried out starting with the crystallographic data obtained from the CD38/**Compound 4** complex.

The result is shown in Fig. 5a and the superimposition of **Compounds 4** and **7** is shown in Fig. 5b. The docking study indicated that the positioning of **Compound 7** at the active site is approximately the same as **Compound 4** as observed in the crystal structure. Besides the same hydrogen bonding of the nicotinamide moieties of **Compound 7** and **4** with the active site,interactions between the nitrogen atom of the quinoline of **Compound 7** with residue Ser186 and π-stacking interaction between the quinoline ring and Trp176 of CD38 were also observed. The similarity of the interactions is consistent with both compounds having inhibitory effects on CD38.

Conclusion

There is a growing tendency to develop non-nucleotide compounds to mimic such signaling molecules.[35] This study represents a rational design of a series of inhibitors of CD38, one of the key enzymes in cellular Ca^{2+} signaling. The design was based on the crystal structure of NAD binding to the active site of CD38 and takes into account the need for membrane permeability. We targeted the nicotinamide portion of the NAD because it interacts strongly with the active site *via* not only hydrogen bonding but also hydrophobic stacking. The reasoning was substantiated by the crystal structure, showing that the nicotinamide portion of

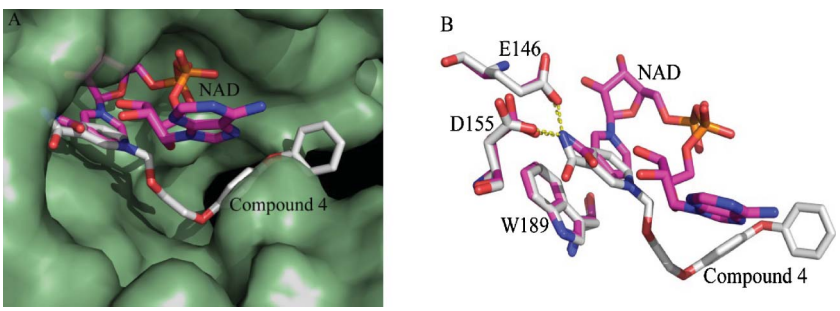

Fig. 4 Structural alignment between CD38–Compound 4 and CD38–NAD complexes. (A) Surface presentation of the active pocket of CD38 (pale green). NAD (sticks presentation in magenta) penetrated to the bottom of the active pocket of CD38, while compound **4** (sticks presentation in grey) floated over the active site. (B) The nicotinamide group of both compound **4** (grey) and NAD (magentas) is similarly positioned and stabilized by the interactions with residues Glu146, Asp155 and Trp189 of CD38.

This journal is © The Royal Society of Chemistry 2011

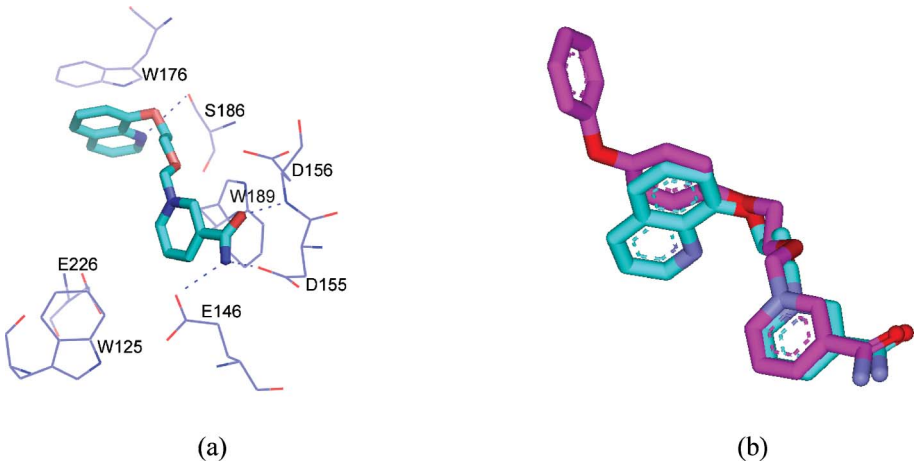

Fig. 5 (a) The molecular dynamics simulation binding mode of compound **7** in the active pocket of human CD38. The carbon atoms of **7** are indicated in cyan. All the nitrogen atoms are blue; oxygen atoms are red. Hydrogen bonds are represented by blue dotted lines. Corresponding residues are labeled and shown in blue lines. (b) Superimposition the binding poses of compound **4** in the enzyme–inhibitor cyrstal with the molecular dynamics simulation result of **7**. **4** is shown as the magenta stick; **7** is shown as the cyan stick.

rat and guinea pig

Compound 4 binds identically as NAD. The replacement of the rest of the highly charged moieties of the NAD with aromatic groups ensures membrane permeability and contributes to the greatly increased *in vivo* potency of the inhibitors. The potency increase is observed both in cultured PC12 cells as we have previously reported[33] and muscle preparations from ~~rats and guinea pigs~~ described here, verifying the general applicability of the new inhibitors. Structure–activity comparison of all the compounds in this series provides clues for the next iteration to produce even more effective inhibitors and set the stage toward developing drug candidates for CD38-related diseases.

Experiment section

Chemistry

All solvents and reagents were obtained from commercial sources and used without further purification unless otherwise stated. HR-ESI-MS (electrospray ionization) was performed with Bruker BIFLEX III. ^{1}H NMR and ^{13}C NMR were recorded with a Bruker AVANCE III 400 or a JEOL AL300 spectrometer. CD_3OD, DMSO-*d*6 or D_2O were used as a solvent. Chemical shifts are reported in parts per million downfield from TMS (^{1}H and ^{13}C). ^{19}F NMR spectra were recorded on a Varian VXR-500 spectrometer. Chemical shifts of ^{19}F NMR are reported in ppm with reference to CF_3COOH as an external standard. Anhydrous solvents were obtained as follows: DMF was dried with CaH_2 at room temperature before being distilled *in vacuo*; ethyl acetate was dried with P_2O_5 before distillation. 1,2-Dichlorethane, ethanol and methanol were distilled over CaH_2.

1-[(2-Acetoxyethoxy)methyl]-3-(aminocarbonyl)-pyridinium chloride (Compound 1). Dry nicotinamide (122 mg, 1 mmol) was dissolved in dry DMF (3 mL), chloromethoxyl ethyl acetate (0.14 mL, 1 mmol) was added under N_2. The mixture was stirred at room temperature for 1 h and a large amount of solid appeared. Dry ethyl acetate (3 ml) was added and the mixture was stirred for 30 min. The white precipitates were collected by filtration and washed with dry ethyl acetate, then recrystallized from EtOH/EA to give the desired **Compound 1** (221 mg, 80%) as a white solid. ^{1}H NMR (300 MHz, CD_3OD) δ 2.03 (s, 3H), 3.98 (m, 2H),4.25 (m, 2H), 6.06 (s, 2H), 8.30 (dd, 1H, J = 7.2, 5.1 Hz), 9.07 (d, 1H, J = 7.2 Hz), 9.21 (d, 1H, J = 5.1 Hz), 9.53 (s, 1H).^{13}C NMR (75 MHz, CD_3OD) δ 20.7, 63.9, 70.8, 90.7, 129.3, 135.8, 144.2, 145.8, 146.5, 165.0, 172.4. ESI-MS: $[M - Cl]^+$: 239.1. Anal. ($C_{11}H_{15}ClN_2O_4 \cdot 0.3H_2O$) C, H, N.

1-[(2-Benzyloxyethoxy)methyl]-3-(aminocarbonyl)-pyridinium chloride (Compound 2). To a solution of 2-(benzyloxy)ethanol (0.85 ml, 6 mmol) in dry 1,2-dichloroethane (8 ml), paraformaldehyde (0.18 g, 6 mmol) was added. Dry HCl gas, obtained *in situ* from H_2SO_4 and NaCl, was bubbled through the reaction mixture over 10 h at 0 °C. The solution was then dried with anhydrous Na_2SO_4, filtered and concentrated under reduced pressure to give a yellow oily residue. The residue was added to a solution of nicotinamide (0.73 g, 6 mmol) in DMF (15 ml). The mixture was stirred at room temperature for 4 h. The white precipitates were collected by filtration and washed with dry ethyl acetate and ethanol, then recrystallized from EtOH by freezing to give the desired **Compound 2** (1.25 g, 65% for two steps) as a white solid. ^{1}H NMR (300 MHz, CD_3OD) δ 3.64 (m, 2H), 3.99 (m, 2H), 4.36 (s, 2H), 6.01 (s, 2H), 7.18–7.32 (m, 5H), 8.05 (dd, 1H, J = 8.1, 6.3 Hz), 8.82 (d, 1H, J = 8.1 Hz), 9.12 (d, 1H, J = 6.3 Hz), 9.45 (s, 1H).^{13}C NMR (75 MHz, CD_3OD) δ 165.0, 146.0, 145.7, 144.1, 139.0, 135.3, 129.5, 129.1, 129.0, 128.9, 128.8, 91.4, 74.2, 73.3, 70.3. ESI-MS: $[M - Cl]^+$ 287.1. Anal. ($C_{16}H_{19}ClN_2O_3$) C, H, N.

1-{[2-(4-Methoxy-phenoxy)ethoxy]methyl}-3-(aminocarbonyl)-pyridinium chloride (Compound 3). 4-Methoxyphenol (0.56 g, 4.5 mmol) was dissolved in 10% sodium hydroxide solution (16 ml, 40 mmol). 2-Chloroethanol (2.68 ml, 40 mmol) was then added and the mixture stirred for 24 h at room temperature. The solution was extracted with CH_2Cl_2. The extract was washed with water three times then dried by evaporation. The product obtained, 2-(4-methoxyphenoxy)ethanol (0.68 g, 4.1 mmol, 90%), was used in the next step directly and dissolved in 1,2-dichloroethane (10 ml). Paraformaldehyde (0.13 g, 4.1 mmol) was added and dry HCl gas was bubbled through the reaction mixture for 10 h at 0 °C.

The solution was then treated as in the synthesis of **Compound 2** and reacted with nicotinamide (0.5 g, 4.1 mmol) in DMF (8 ml). The mixture was stirred at room temperature for 8 h. The white precipitates were collected by filtration and washed with dry ethyl acetate and ethanol. The crude product was recrystallized from EtOH/EA to obtain the desired **Compound 3** (1.14 g, 82% for two steps) as a white solid. ^{1}H NMR (300 MHz, CD_3OD) δ 3.72 (s, 3H), 4.11 (m, 4H), 6.11 (s, 2H), 6.72–6.83 (m, 4H), 8.23 (dd, 1H, J = 8.4, 6.0 Hz), 8.99 (dt, 1H, J = 8.4, 1.5 Hz), 9.22 (d, 1H, J = 6.0 Hz), 9.55 (s, 1H).^{13}C NMR (75 MHz, CD_3OD) δ 165.0, 155.8, 153.5, 146.3, 145.7, 144.2, 135.5, 129.1, 91.2, 72.3, 68.5, 56.0. ESI-MS: $[M - Cl]^+$ 303.1. Anal. ($C_{16}H_{19}ClN_2O_4$) C, H, N.

1-{[2-(4-Phenoxy-phenoxy)ethoxy]methyl}-3-(aminocarbonyl)-pyridinium chloride (Compound 4). The procedure used was similar to that for the synthesis of **Compound 3**. 4-Phenoxyphenol was condensed with 2-chloroethanol in 83% yield. The alcohol obtained was chloromethylated and reacted with nicotinamide successively to yield **Compound 4** (71.5% for two steps). ^{1}H NMR (300 MHz, CD_3OD) δ 4.07–4.15 (m, 4H), 6.13 (s, 2H), 6.82–6.93 (m, 6H), 7.04 (t, 1H, J = 7.5 Hz) 7.29 (dd, 2H, J = 8.5, 7.5 Hz) 8.26 (dd, 1H, J = 8.1, 6.0 Hz), 9.02 (d, 1H, J = 8.1 Hz), 9.24 (d, 1H, J = 6.0 Hz), 9.58 (s, 1H).^{13}C NMR (75 MHz, CD_3OD) δ 165.0, 159.7, 155.7, 152.2, 146.3, 145.7, 144.2, 135.6, 130.8, 129.1, 123.8, 121.6, 118.8, 116.7, 91.1, 72.2, 68.5. ESI-MS: $[M - Cl]^+$ 365.1. Anal. ($C_{21}H_{21}ClN_2O_4$) C, H, N.

1-{[2-(4-Nitro-phenoxy)ethoxy]methyl}-3-(aminocarbonyl)-pyridinium chloride (Compound 5). The procedure used was similar to that for the synthesis of **Compound 3**. 4-Nitrophenol was condensed with 2-chloroethanol in 87% yield. The alcohol obtained was chloromethylated and reacted with nicotinamide successively to yield the **Compound 5** (82% for two steps). ^{1}H NMR (300 MHz, CD_3OD) δ 4.19 (m, 2H), 4.32 (m,2H), 6.14 (s, 2H), 7.05 (d, J_{AB} = 9.3 Hz,2H,A of aryl A_2B_2), 8.18 (d, J_{AB} = 9.3 Hz,2H,B of aryl A_2B_2), 8.30 (dd, 1H, J = 8.1, 6.0 Hz), 9.05 (d, 1H, J = 8.1 Hz), 9.25 (d, 1H, J = 6.0 Hz), 9.58 (s, 1H).^{13}C NMR (75 MHz, CD_3OD) δ 165.0, 164.8, 146.5, 145.8, 144.2, 143.1, 135.7, 129.3, 129.2, 126.8, 115.8, 90.9, 71.4, 68.8. ESI-MS: $[M - Cl]^+$ 318.1. Anal. ($C_{15}H_{16}ClN_3O_5$) C, H, N.

1-{[2-(3-Trifluoromethyl-phenoxy)ethoxy]methyl}-3-(aminocarbonyl)-pyridiniumchloride (Compound 6). The procedure follows the synthesis of **Compound 3**. 3-Trifluoromethylphenol was condensed with 2-chloroethanol in 95% yield. The alcohol obtained was chloromethylated and reacted with nicotinamide successively to yield the **Compound 6** (40% for two steps). ^{1}H NMR (300 MHz, CD_3OD) δ 4.16–4.25 (m, 4H), 6.13 (s, 2H), 7.12–7.25 (m, 3H), 7.45 (m, 1H) 8.27 (dd, 1H, J = 8.1, 6.0 Hz), 9.03 (dt, 1H, J = 8.1, 1.5 Hz), 9.24 (d, 1H, J = 6.0 Hz), 9.59 (s, 1H). ^{13}C NMR (100 MHz, CD_3OD) δ 164.9, 160.0, 146.4, 145.8, 144.2, 135.7, 132.9 (q, J_{CF} = 32 Hz), 131.6, 129.2, 125.4 (q, $^1J_{CF}$ = 270 Hz), 119.3, 118.8 (q, J_{CF} = 4 Hz), 112.4 (q, J_{CF} = 4 Hz), 91.0, 71.8, 68.4. ^{19}F NMR (470 MHz, CD_3OD) δ 21.3. ESI-MS: $[M - Cl]^+$ 341.1. Anal. ($C_{16}H_{16}ClF_3N_2O_3$) C, H, N.

1-{[2-(8′-Quinolyloxy)ethoxy]methyl}-3-(aminocarbonyl)-pyridinium chloride (Compound 7). The procedure follows the synthesis of **Compound 3**. 8-Hydroxyqunoline was condensed with 2-chloroethanol in 65% yield. A suspension of 2-(8′-quinolinoxy)ethanol (1.28 g, 6.77 mmol), paraformaldehyde (0.2 g, 6.77 mmol) and 1.5 g 3 Å MS in 10 ml 1,2-dichloroethane was bubbled with HCl gas for 10 h at 0 °C. The molecular sieve was filtered and washed with DCE, the filtrate was concentrated under reduced pressure and treated with nicotinamide as before. After recrystallized from MeOH/EA, **Compound 7** was obtained as a yellow solid. (78% for two steps). ^{1}H NMR (300 MHz, CD_3OD) δ 4.36 (t, 2H, J = 4.2 Hz), 4.67 (m, 2H, J = 4.2 Hz), 6.19 (s, 2H), 7.70 (dd, 1H, J = 6.0, 2.7 Hz), 7.91 (m, 2H), 8.16 (dd, 1H, J = 8.4, 5.7 Hz), 8.25 (dd, 1H, J = 8.1, 6.0 Hz), 9.00 (d, 1H, J = 8.1 Hz), 9.18–9.27 (m, 3H), 9.58 (s, 1H).^{13}C NMR (75 MHz, CD_3OD) δ 164.9, 150.0, 148.5, 146.2, 145.9, 145.5, 144.1, 135.7, 131.8, 131.7, 131.0, 129.3, 123.8, 122.0, 115.3, 90.7, 71.1, 70.0. ESI-MS: $[M - Cl]^+$ 324.2. Anal. ($C_{18}H_{18}ClN_3O_3\cdot 3H_2O$) C, H, N.

1,2-Dimethoxy-ethylene-bis-*N*,*N*′-3-(aminocarbonyl)-pyridinium dichloride (Compound 8). 1,2-Bis-chloromethoxy-ethane was prepared as described in the literature.[29] The bis-chloromethylation product (0.78 ml, 5 mmol) was added to a solution of nicotinamide (1.34 g, 11 mmol) in 20 ml DMF. The mixture was stirred for 12 h at room temperature. Dry ethyl acetate (10 ml) was added and the mixture was stirred a further 30 min. The white precipitate was collected by filtration and washed with dry ethyl acetate and ethanol to give the desired **Compound 8** (1.71 g, 85%) as a white solid. ^{1}H NMR (300 MHz, D_2O) δ 3.80 (s, 4H), 5.87 (s, 4H), 8.11 (dd, 2H, J = 8.1, 6.3 Hz), 8.84 (d, 2H, J = 8.1 Hz), 8.96 (d, 2H, J = 6.3 Hz), 9.26 (s, 2H). ^{13}C NMR (75 MHz, CD_3OD) δ 165.5, 146.5, 146.0, 144.4, 135.9, 129.4, 90.7, 71.4. ESI-MS: $[M - Cl]^+$ 367.1. Anal. ($C_{16}H_{20}Cl_2N_4O_4\cdot 2H_2O$) C, H, N.

1,4-Dimethoxy-butylene-bis-*N*,*N*′-3-(aminocarbonyl)-pyridinium dichloride (Compound 9). The same procedure as for **Compound 8** was followed to afford the desired **Compound 9** (52.7% for two steps). ^{1}H NMR (300 MHz, D_2O) δ 1.57 (s, 4H), 3.58 (s, 4H), 5.86 (s, 4H), 8.14 (dd, 2H, J = 8.4, 6.0 Hz), 8.86 (d, 2H, J = 8.4 Hz), 8.99 (d, 2H, J = 6.0 Hz), 9.26 (s, 2H). ^{13}C NMR (125 MHz, CD_3OD) δ 165.1, 146.5, 145.8, 144.2, 135.8, 129.4, 91.0, 72.4, 26.8. ESI-MS: $[M - Cl]^+$ 395.1. Anal. ($C_{18}H_{24}Cl_2N_4O_4\cdot 1.4H_2O$) C, H, N

1,4-Dimethoxy-butyne-bis-*N*,*N*′-3-(aminocarbonyl)-pyridinium dichloride (Compound 10). The same procedure as for **Compound 8** was followed to afford the desired **Compound 10** (46% for two steps). ^{1}H NMR (300 MHz, CD_3OD) δ 4.48 (s, 4H), 6.10 (s, 4H), 8.31 (dd, 2H, J = 8.1, 6.3 Hz), 9.09 (dt, 2H, J = 8.1, 1.5 Hz), 9.25 (d, 2H, J = 6.3 Hz), 9.61 (s, 2H). ^{13}C NMR (75 MHz, CD_3OD) δ 165.1, 146.8, 146.6, 145.0, 135.7, 129.3, 90.0, 83.7, 59.8. ESI-MS: $[M - Cl]^+$ 391.1. Anal. ($C_{18}H_{20}Cl_2N_4O_4\cdot 0.8H_2O$) C, H, N.

1,4-Dimethoxy-hexamethylene-bis-*N*,*N*′-3-(aminocarbonyl)-pyridinium dichloride (Compound 11). The same procedure as for **Compound 8** was followed to afford the desired **Compound 11** (52% for two steps). ^{1}H NMR (300 MHz, CD_3OD) δ 1.40 (m, 4H), 1.67 (m, 4H), 3.69 (t, 4H, J = 6.3 Hz), 6.01 (s, 4H), 8.29 (dd, 2H, J = 8.4, 6.3 Hz), 9.07 (dt, 2H, J = 8.4, 1.5 Hz), 9.20 (d, 2H, J = 6.3 Hz), 9.50 (s, 2H). ^{13}C NMR (75 MHz, CD_3OD) δ 165.1, 146.5, 145.8, 144.2, 135.8, 129.3, 91.0, 72.6, 30.2, 26.6. ESI-MS: $[M - Cl]^+$ 423.2. Anal. ($C_{20}H_{28}Cl_2N_4O_4$) C, H, N.

(*E*)-1-{[4-(8′-Quinolyloxy)but-2-enyloxy]methyl}-3-(aminocarbonyl)-pyridinium chloride (Compound 12). To a solution of 1,4-butenediol (0.88 g, 10 mmol), 8-hydroxyquinoline (0.725 g, 5 mmol) and triphenylphosphine (PPh_3) (1.57 g, 6 mmol) in

This journal is © The Royal Society of Chemistry 2011

THF (25 ml), diisopropyl azodicarboxylate (1.21 g, 6 mmol) was added dropwise. The reaction was stirred for 4 h at room temperature and refluxed for 12 h. The solution was concentrated under reduced pressure. The crude mixture was purified by flash column chromatography (2 : 1–3 : 1 hexanes : ethyl acetate eluent) to furnish pure alcohol (0.72 g, 70%). The alcohol was chloromethylated and treated with nicotinamide as in the synthesis of **Compound 7**. After recrystallized from MeOH/EA, **Compound 12** was obtained as a yellow-green solid (78% for two steps). ^{1}H NMR (500 MHz, D_2O) δ 4.50 (d, 2H, J = 7.0 Hz), 4.94 (d, 2H, J = 6.5 Hz), 5.99 (m, 1H), 6.09 (s, 2H), 7.50 (d, 1H, J = 6.5 Hz), 7.86 (m, 2H), 8.11 (dd, 1H, J = 8.0, 5.5 Hz), 8.25 (t, 1H, J = 7.0 Hz), 8.91 (d, 1H, J = 8.5 Hz), 9.03 (d, 1H, J = 5.0 Hz), 9.12 (d, 1H, J = 8.5 Hz), 9.19 (d, H, J = 6.5 Hz), 9.40 (s, 1H). ^{13}C NMR (125 MHz, D_2O) δ 165.8, 148.6, 148.0, 146.3, 145.6, 143.9, 143.4, 134.4, 131.2, 130.6, 130.1, 130.0, 129.3, 128.8, 123.1, 121.3, 114.9, 89.6, 67.2, 66.0. ESI-MS: $[M - Cl]^+$ 350.2. Anal. ($C_{20}H_{20}ClN_3O_3 \cdot 3H_2O$) C, H, N.

1-{[2-(4-Phenoxy-phenoxy)ethoxy]methyl}-6-(aminocarbonyl)-quinolinium chloride (Compound 13). The corresponding alcohol was chloromethylated as in **Compound 4** and reacted with quinoline-6-carboxamide successively to yield **Compound 13** (63% for two steps).^{1}H NMR (300 MHz, DMSO) δ 4.07 (s, 4H), 5.77 (s, 2H), 6.54 (s, 2H), 6.73–7.38 (m, 9H) 7.93 (s, 1H), 8.31 (dd, 1H, J = 8.4, 5.7 Hz), 8.53 (s, 1H), 8.65 (s, 2H), 9.00 (s, 1H), 9.44 (d, 1H, J = 8.4 Hz), 9.78 (s, 1H). ^{13}C NMR (125 MHz, D_2O) δ 169.8, 160.1, 155.6, 152.3, 151.5, 150.5, 141.3, 136.8, 135.3, 131.4, 131.3, 130.8, 123.8, 123.5, 121.5, 121.0, 118.8, 116.6, 89.2, 71.7, 68.6. ESI-MS: $[M - Cl]^+$ 415.2. Anal. ($C_{25}H_{23}ClN_2O_4 \cdot 1.4H_2O$) C, H, N.

1-{[2-(4-Phenoxy-phenoxy)ethoxy]methyl}-3-(aminocarbonyl)-4-amino-pyridinium chloride (Compound 14). The corresponding alcohol was chloromethylated as in **Compound 4** and reacted with 4-aminonicotinamide successively to yield the **Compound 14** (43% for two steps). ^{1}H NMR (300 MHz, DMSO) δ 3.92 (s, 2H), 4.10 (s, 2H), 5.55 (s, 2H), 6.90–7.10 (m, 8H), 7.35 (t, 2H, J = 7.6 Hz), 7.91 (s, 1H), 8.30 (d, 2H, J = 6.9 Hz), 8.43 (bs, 1H), 9.11 (m, 3H). ^{13}C NMR (100 MHz, DMSO) δ 166.5, 158.6, 157.9, 154.4, 149.6, 143.9, 141.6, 129.9, 122.7, 120.6, 117.3, 115.7, 112.0, 110.3, 85.7, 68.0, 66.9. ESI-MS: $[M - Cl]^+$ 380.2. Anal. ($C_{21}H_{22}ClN_3O_4 \cdot 0.5H_2O$) C, H, N.

Experimental details for the antagonist assay

Recombinant CD38 was prepared by a yeast expression system as described in ref. 36. Inhibitors were dissolved in 50 mM Hepes buffer (pH 7), except **Compound 5**, which was dissolved in 50% DMSO (v/v). Recombinant CD38 (0.04 μg ml^{-1}) and BSA (50 μg ml^{-1}) were mixed with different concentrations of the inhibitors and incubated for 1 h at room temperature. NAD (2 μM) was added to initiate the reactions and aliquots ~~of~~ were collected at t = 0, 4, 8 and 12 min, ~~respectively~~. The aliquots were immediately stopped with an equal volume of 0.6 M HCl followed by neutralization with two volumes of 0.5 M sodium phosphate buffer (pH 8). The amounts of NAD in the samples were measured by ~~the~~ coupled enzyme assay.[31] The percentages of inhibition of the NADase activity as compared to the control without the inhibitor were plotted against various concentrations of the inhibitor to obtain the IC_{50} value.

Biological effects on muscle preparations from rat and guinea pigs

1. Materials and methods. Animals: Male Sprague–Dawley rats weighing 250–300 g were supplied from the Laboratory Animal Unit of the University of Hong Kong. Some male Sprague–Dawley rats were also purchased from the Laboratory Animal Center of Peking University Health Science Center (Beijing, China). Rats were anesthetized by pentobarbitone sodium (50 mg kg^{-1}, by intraperitoneal injection) and then sacrificed by cervical dislocation. All experiments performed in this study were approved by the Committee on the Use of Live Animals in Teaching and Research of the University of Hong Kong and by the Beijing animal committee with the confirmation number: SCXK (Jing) 2006-0008.

Male Hartley guinea pigs were purchased from Beijing Fangyuanyuan Laboratory Animal Company and approved by the local animal committee with the confirmation number: SCXK (Jing) 2009-0014. Animals were housed under standard conditions (temperature 22 ± 2 °C, relative humidity 55 ± 5%, 12 h light/dark cycle) with food and water available *ad libitum*. In the present study, all experiments were performed under the guidelines of the Experimental Laboratory Animal Committee of Peking University Health Science Center and were in strict accordance with the principles and guidelines of the National Institutes of Health Guide for the Care and Use of Laboratory Animals. Reagents: phenylephrine (Phe) and acetylcholine chloride (ACh) were purchased from Sigma Chemicals (St. Louis, MO, USA). All chemicals (including compound **4**, **7** and compound **9**) were dissolved in miliQ water.

2. Tension measurement on isolated rat aortic ring preparations. The thoracic aorta was excised. After the surrounding connective tissue had been carefully cleaned off, four 3 mm wide ring segments were prepared from each aorta. Each was dispensed between two stainless wire hooks in a 5 mL organ bath. The upper wire was connected to a force-displacement transducer (RM6240 system, Chengou Instrument Factory) and the lower one was fixed at the bottom of the organ bath. The organ bath was filled with Krebs solution of the following composition (in mM): 119 NaCl, 4.7 KCl, 25 $NaHCO_3$, 2.5 $CaCl_2$, 1 $MgCl_2$, 1.2 KH_2PO_4, and 11 D-glucose. The bathing solution was gassed with 95% O_2–5% CO_2 at 37 °C (pH ≈ 7.4). The rings were placed under an optimal basal tone of 15 mN, determined from previous length–tension experiments. Changes in isometric tension were measured with a Grass force transducer and stored on RM6240 software for later data analysis. Twenty minutes after mounting in organ baths, the rings were first contracted with 0.3 μM phenylephrine (Phe) to test the contractility and then relaxed by 1 μM ACh. They were rinsed several times until baseline tone was restored. The rings were thereafter allowed to equilibrate for 60 min. Baseline tone was readjusted to 15 mN when necessary. Each set of experiments was performed on rings prepared from different rats. The use of laboratory animals was approved by the Animal Research Ethical Committee of the University of Hong Kong.

In ~~the~~ set of experiments, relaxation of Phe (1 μM)-contracted endothelium-intact rings was induced by compound **4** (30–300 μM) or compound **9** (30–300 μM) or nicotinamide (0.01–6 mM).

The relaxant effects of the vasodilators were expressed as 100 minus percentage reduction from the Phe-induced contractile

a

this

response. Non-linear regression curve fitting was performed on individual cumulative concentration–response curves (GraphPad software, Version 5.0). pD2 values (IC_{50}) were calculated as negative log molar of dilator that induced 50% of the maximal relaxation. All data were shown as means ± SEM. Statistical significance was determined by two-tailed Student's t-test or one-way ANOVA followed by the Newman–Keuls test when more than two treatments were compared. A P value of less than 0.05 was regarded as significant.

3. Tension measurement on isolated tracheal strips of guinea pigs. Guinea pigs weighing 250–350 g were sacrificed by an overdose of sodium pentobarbital (75 mg kg^{-1} intraperitoneally). The tracheas were removed and placed in ice-cold Krebs–Henseleit solution bubbled through with 95% O_2/5% CO_2. The trachea was then isolated from surrounding connective tissue and cut spirally into two strips 3 mm wide and 15 mm long. The composition of Krebs–Henseleit solution was (in mM): NaCl 118.00, KCl 4.70, $CaCl_2$ 2.50, $MgSO_4 \cdot 7H_2O$ 1.20, KH_2PO_4, 1.20, $NaHCO_3$ 25.00, and glucose 11.00. The ends of each tracheal strip were then fixed, *via* two small clips, to the bottom of the chamber and to a force displacement transducer for recording tension with a polygraph. The chamber (50 mL capacity) was filled with Krebs–Henseleit solution at 37 °C and bubbled through with 95% O_2/5% CO_2. Each strip was subjected to a load of 2 g for at least 1 h, with frequent changes of the bath fluid until a stable baseline tension was obtained. 10 μM acetylcholine chloride was added into the Krebs–Henseleit solution to induce contraction of tracheal strips. After the tension become stable, compound **4** and compound **7** of 10^{-8}, 10^{-7}, 10^{-6}, 10^{-5} and 10^{-4} M were added every 10 min in sequence, respectively. The tension of tracheal strips was recorded by MedLab-U4C501H bio-signals collecting–processing system in the whole experiment.[37]

4. Statistical evaluation. Antispasmodic percentage = (tension before addition of compounds − tension after addition of compounds)/(tension before given compounds − basal tension) × 100%. Tension changes of tracheal strips obtained from administration groups and the blank group were compared using Student's t test. All values are represented as mean ± SEM. Two means were considered significantly different when P value was <0.05 or <0.01.

Protein crystallography

The catalytic domain of human CD38 was expressed in a yeast expression system and purified as reported previously.[36] Using the hanging vapor diffusion method, CD38 crystals were obtained by mixing 1 μl 10 mg ml^{-1} protein with 1 μl crystallization solution containing 100 mM MES, pH 6.0, 10% PEG4000 at room temperature. To obtain CD38–Compound **4** complex, native CD38 crystals were soaked for several minutes at room temperature in the crystallization mother liquid ~~containing~~ 40 mM Compound 4 and 30% glycerol.

Data collection, reduction and structure refinement. All X-ray diffraction data were collected at the Cornell High-Energy Synchrotron Source (CHESS) A1 station under cryo-protection at 100 K with a fixed wavelength of 0.976 Å. A total of 360 images with an oscillation angle of 1° each were collected for each crystal using a Quantum Q-210 CCD detector. The complete data sets were processed using the program package ~~DENZO/SCALEPACK~~.[38] The crystallographic statistics are listed in Table 1. The shCD38 apo structure served as the initial model for structure solution with the method of molecular replacement. Subsequent crystallographic refinements were done with the program REFMAC5.[39] All substrates and products were built using the Program COOT.[38]

Computer simulation of compound 7 for the docking to CD38

The structure of **Compound 7** first was constructed based upon the crystal coordinates of **Compound 4** followed by energy minimization using Discovery Studio 2.1. It was then docked into the binding pocket of CD38 using the AutoDock 3.0.5[40] program. Considering the interactions with the key residues in CD38, one conformation with a relatively low energy was selected as the starting conformation for the subsequent molecular dynamics simulation. The molecular topology file for **Compound 7** was generated by the PRODRG2[41] server (http://davapc1.bioch.dundee.ac.uk/prodrg/). The partial atomic charges of the compound were calculated by Gaussian03 program[42] at the level of HF/6-31G*. The simulations were performed with the GROMACS[43] (version: 3.3.1) software and the force field GROMOS96[44] 43a1 was applied for the protein. The complex was put into a cubic periodic box with edge approximately 10 Å from the system's periphery in each dimension. Then 19 974 SPC water molecules were added into the box and 2 Cl^- were also added in order to ensure the charge neutrality of the system. The final system contains 62 601 atoms. During the entire simulation, all bond lengths were constrained by the LINCS algorithm.[45] Long-range electrostatic interactions were calculated using the PME method.[46] The Berendsen thermostat[47] was applied using a coupling time of 0.1 ps to maintain the systems at a constant temperature of 300 K and the pressure was also maintained by coupling to a reference pressure of 1 bar by Berendsen thermostat. The simulations began with 2000 steps of steepest-descent algorithm to reach the tolerance. Then, the solvent equilibration was performed in 50 ps with the protein and the ligand fixed. Following that, a second 50 ps simulation was carried out with the main chain and the ligand fixed. Another 20 ps simulation was used to relax the whole system except for the C_α atoms and the ligand. The equilibration was completed after the 10 ps relaxation for the ligand. Finally, the production simulation of 5 ns was performed on the whole system. The system was equilibrated after about 2 ns and the average structure was obtained and minimized, which was considered as the stable binding mode of **Compound 7**.

Acknowledgements

This study was supported by grants from the National Natural Sciences Foundation of China to LH Zhang (**NSFC-RGC 20831160506**), and the NSFC/RGC grant N_HKU 722/08 and General Research Fund of Hong Kong: 769107, 768408, 769309, 770610 (to H.C. Lee and Q Hao).

References

1 E. L. Reinherz, P. C. Kung, G. Goldstein, R. H. Levey and S. F. Schlossman, Discrete stages of human intrathymic differentiation: analysis of normal thymocytes and leukemic lym-

This journal is © The Royal Society of Chemistry 2011

phoblasts of T-cell lineage, *Proc. Natl. Acad. Sci. U. S. A.*, 1980, **77**, 1588–1592.
2 H. C. Lee, Enzymatic functions and structures of CD38 and homologs., *Chem. Immunol.*, 2000, **75**, 39–59.
3 (*a*) H. C. Lee, Physiological functions of cyclic ADP-ribose and NAADP as calcium messengers, *Annu. Rev. Pharmacol.*, 2001, **41**, 317–345; (*b*) H. C. Lee, R. Aarhus and D. Levitt, The crystal structure of cyclic ADP-ribose, *Nat. Struct. Biol.*, 1994, **1**, 143–144; (*c*) H. C. Lee, T. F. Walseth and G. T. Bratt *et al.*, Structural determination of a cyclic metabolite of NAD^+ with intracellular Ca^{2+}-mobilizing activity, *J. Biol. Chem.*, 1989, **264**, 1608–15.
4 M. Howard, J. C. Grimaldi, J. F. Bazan, F. E. Lund, L. Santos-Argumedo, R. M. Parkhouse, T. F. Walseth and H. C. Lee, Formation and hydrolysis of cyclic ADP-ribose catalyzed by lymphocyte antigen CD38, *Science*, 1993, **262**, 1056–1059.
5 I. Kato, Y. Yamamoto, M. Fujimura, N. Noguchi, S. Takasawa and H. Okamoto, CD38 disruption impairs glucose-induced increases in Cyclic ADP-ribose, $[Ca^{2+}]_i$, and insulin secretion, *J. Biol. Chem.*, 1999, **274**, 1869–1872.
6 S. Partida-Sanchez, D. A. Cockayne, S. Monard, E. L. Jacobson, N. Oppenheimer, B. Garvy, K. Kusser, S. Goodrich, M. Howard, A. Harmsen, T. D. Randall and F. E. Lund, Cyclic ADP-ribose production by CD38 regulates intracellular calcium release, extracellular calcium influx and chemotaxis in neutrophils and is required for bacterial clearance in vivo, *Nat. Med.*, 2001, **7**, 1209–1216.
7 G. Shubinsky and M. Schlesinger, The CD38 lymphocyte differentiation marker: new insight into its ectoenzymatic activity and its role as a signal transducer, *Immunity*, 1997, **7**, 315–324.
8 M. Mitsui-Saito, I. Kato, S. Takasawa, H. Okamoto and T. Yanagisawa, CD38 gene disruption inhibits the contraction induced by alphaa-drenoceptor stimulation in mouse aorta, *J. Vet. Med. Sci.*, 2003, **65**, 1325–1330.
9 Y. Fukushi, I. Kato, S. Takasawa, T. Sasaki, B. H. Ong, M. Sato, A. Ohsaga, K. Sato, K. Shirato, H. Okamoto and Y. Maruyama, Identification of cyclic ADP-ribose-dependent mechanisms in pancreatic muscarinic Ca^{2+} signaling using CD38 knockout mice, *J. Biol. Chem.*, 2001, **276**, 649–655.
10 S. Partida-Sanchez, S. Goodrich, K. Kusser, N. Oppenheimer, T. D. Randall and F. E. Lund, Regulation of dendritic cell trafficking by the ADPribosyl cyclase CD38: impact on the development of humoral immunity, *Immunity*, 2004, **20**, 279–291.
11 L. Sun, J. Iqbal, S. Dolgilevich, T. Yuen, X. B. Wu, B. S. Moonga, O. A. Adebanjo, P. J. Bevis, F. Lund, C. L. Huang, H. C. Blair and M. Zaidi, Disordered osteoclast formation and function in a CD38 (ADP-ribosyl cyclase)-deficient mouse establishes an essential role for CD38 in bone resorption, *FASEB J.*, 2003, **17**, 369–375.
12 J. D. Johnson, E. L. Ford, E. Bernal-Mizrachi, K. L. Kusser, D. S. Luciani, Z. Han, H. Tran, T. D. Randall, F. E. Lund and K. S. Polonsky, Suppressed insulin signaling and increased apoptosis in CD38-null islets, *Diabetes*, 2006, **55**, 2737–2746.
13 D. Jin, H. X. Liu and H. Hirai *et al.*, CD38 is critical for social behaviour by regulating oxytocin secretion, *Nature*, 2007, **446**, 41–45.
14 S. Deaglio, T. Vaisitti, S. Aydin, E. Ferrero and F. Malavasi, In-tandem insight from basic science combined with clinical research: CD38 as both marker and key component of the pathogenetic network underlying chronic lymphocytic leukemia, *Blood*, 2006, **108**, 1135–1144.
15 F. Morabito, R. N. Damle, S. Deaglio, M. Keating, M. Ferrarini and N. Chiorazzi, The CD38 ectoenzyme family: advances in basic science and clinical practice, *Mol. Med.*, 2006, **12**, 342–344.
16 H. C. Lee, Mechanisms of calcium signaling by cyclic ADPribose and NAADP, *Physiol. Rev.*, 1997, **77**, 1133–1164.
17 R. Graeff, Q. Liu, I. A. Kriksunov, Q. Hao and H. C. Lee, Acidic residues at the active sites of CD38 and ADP-ribosyl cyclase determine nicotinic acid adenine dinucleotide phosphate (NAADP) synthesis and hydrolysis activities, *J. Biol. Chem.*, 2006, **281**, 28951–28957.
18 J. T. Slama and A. M. Simmons, Carbanicotinamide adenine dinucleotide: synthesis and enzymological properties of a carbocyclic analogue of oxidized nicotinamide adenine dinucleotide, *Biochemistry*, 1988, **271**, 183–193.
19 K. A. Wall, M. Klis, J. Kornet, D. Coyle, J. C. Amé, M. K. Jacobson and J. T. Slama, Inhibition of the intrinsic NAD^+ glycohydrolase activity of CD38 by carbocyclic NAD analogues, *Biochem. J.*, 1998, **335**, 631–636.
20 H. M. Muller-Steffner, O. Malver, L. Hosie, N. J. Oppenheimer and F. Schuber, Slow-binding Inhibition of NAD^+ Glycohydrolase by Arabino Analogues of α-NAD, *J. Biol. Chem.*, 1992, **267**, 9606–9611.
21 A. A. Sauve, H. T. Deng, R. H. Angeletti and V. L. A Schramm, Covalent Intermediate in CD38 Is Responsible for ADP-Ribosylation and Cyclization Reactions, *J. Am. Chem. Soc.*, 2000, **122**, 7855–7859.
22 (*a*) Q. Liu, R. Graeff and I. A. Kriksunov *et al.*, Structural basis for enzymatic evolution from a dedicated ADP-ribosyl cyclase to a multifunctional NAD hydrolase, *J. Biol. Chem.*, 2009, **284**, 27637–27645; (*b*) Q. Liu, I. A. Kriksunov, H. Jiang, R. Graeff, H. Lin, H. C. Lee and Hao Q., Covalent, and noncovalent intermediates of an NAD utilizing enzyme, human CD38, *Chem. Biol.*, 2008, **15**, 1068–1078.
23 A. A. Sauve and V. L. Schramm, Mechanism-Based, Inhibitors of CD38: A Mammalian Cyclic ADP-Ribose Synthetase, *Biochemistry*, 2002, **41**, 8455–8463.
24 (*a*) Q. Liu, I. A. Kriksunov and R. Graeff *et al.*, Crystal structure of human CD38 extracellular domain, *Structure*, 2005, **13**, 1331–1339; (*b*) Q. Liu, I. A Kriksunov, R. Graeff, C. Munshi, H. C. Lee and Q. Hao, Structural basis for the mechanistic understanding of human CD38-controlled multiple catalysis, *J. Biol. Chem.*, 2006, **281**, 32861–32869; (*c*) Q. Liu, I. A. Kriksunov, C. Moreau, R. Graeff, B. V. Potter, H C. Lee and Q. Hao, Catalysis-associated conformational changes revealed by human CD38 complexed with a non-hydrolyzable substrate analog, *J. Biol. Chem.*, 2007, **282**, 24825–24832.
25 S. Broussy, Y. Coppel, M. Nguyen, J. Bernadou and B. Meunier, ^1H and ^{13}C NMR characterization of hemiamidal isoniazid-NAD(H) adducts as possible inhibitors of InhA reductase of mycobacterium tuberculosis, *Chem.–Eur. J.*, 2003, **9**, 2034–2038.
26 J. Pernak, J. Kalewska, H. Ksycinska and J. Cybulski, Synthesis and anti-microbial activities od some pyridinium salts with alkoxymethyl hydrophobic group, *Eur. J. Med. Chem.*, 2001, **36**, 899–907.
27 S. Saluja, R. Zou, J. C. Drach and L. B. Townsend, Structure–Activity Relationships among 2-Substituted 5,6-Dichloro-,4,6-Dichloro-,and 4,5-Dichloro-1-[(2- hydroxyethoxy)methyl]-and-1-[(1,3-dihydroxy-2-propoxy)methyl] benzimidazoles, *J. Med. Chem.*, 1996, **39**, 881–891.
28 S. Inokuma, K. Kimura, T. Funaki and J. Nishimura, Synthesis of pyridinecrown ophanes exhibiting high Ag^+-affinity, *Heterocycles*, 2001, **54**, 123–130.
29 G. Y. Yang, K. A. Oh, N. J. Park and Y. S. Jung, New oxime reactivators connected with $CH_2O(CH_2)nOCH_2$ linker and their reactivation potency for organophosphorus agents-inhibited acetylcholinesterase, *Bioorg. Med. Chem.*, 2007, **15**, 7704–7710.
30 M. Y. Jang, S. De. Jonghe, L. J. Gao and P. Herdewijn, Regioselective cross-coupling reactions and nucleophilic aromatic substitutions on a 5,7-dichloropyrido[4,3-*d*]pyrimidine scaffold, *Tetrahedron Lett.*, 2006, **47**, 8917–8920.
31 R. Graeff and H. C. Lee, A novel cycling assay for cellular cADP-ribose with nanomolar sensitivity, *Biochem J.*, 2002, **361**, 379–384.
32 Z. D. Ge, D. X. Zhang, Y. F. Chen, F. X. Yi, A. P. Zou, W. B. Campbell and P. L. Li, Cyclic ADP-ribose contributes to contraction and Ca^{2+} Release by M1 muscarinic receptor activation in coronary arterial smooth muscle, *J. Vasc. Res.*, 2003, **40**, 28–36.
33 J. Yue, W. Wei, C. M. C. Lam, Y. J. Zhao, M. Dong, L. R. Zhang, L. H. Zhang and H. C. Lee, The CD38/cADPR/Ca^{2+}-pathway promotes cell proliferation and delays NGF-induced differentiation in PC12 cells, *J. Biol. Chem.*, 2009, **284**, 29335–29242.
34 (*a*) A. Deepak, T. A. Deshpande and S. D. White, *et al.*, CD38/cyclic ADP-ribose signaling: role in the regulation of calcium homeostasis in airway smooth muscle, *Am. J. Physiol.: Lung Cell. Mol. Phys.*, 2005, **288**, 773–788; (*b*) G. T. Stevenson, CD38 as a therapeutic target, *Mol. Med.*, 2006, **12**, 345–346.
35 E. Naylor, A. Arredouani, S. R. Vasudevan, A. M. Lewis, R. Parkesh, A. Mizote, D. Rosen, J. M. Thomas, M. Izumi, A Ganesan, A Galione and G. C. Churchill, Identification of a chemical probe for NAADP by virtual screening, *Nat. Chem. Biol.*, 2009, **5**, 220–226.
36 H. C. Lee and C. B. Munshi, Large scale production of human CD38 in yeast by fermentation, *Methods Enzymol.*, 1997, **280**, 230–241.
37 K. Hirota, E. Hashiba, H. Yoshioka, S. Kabara and A. Matsuki, Effects of three different L-type Ca^{2+} entry blockers on airway constriction induced by muscarinic receptor stimulation, *Br. J. Anaesth.*, 2003, **90**, 671–675.
38 Z. Otwinowski and W. Minor, Processing of X-ray Diffraction Data Collected in Oscillation Mode, *Methods Enzymol.*, 1997, **276**, 307–326.
39 Collaborative Computational Project, Number 4. The CCP4 Suite:

Programs for Protein Crystallography , *Acta Crystallogr., Sect. D: Biol. Crystallogr.*, 1994, **D50**, pp. 760–763.
40 G. M. Morris, D. S. Goodsell, R. S. Halliday, R. Huey, W. E. Hart, R. K. Belew and A. J. Olson, Automated docking using a Lamarckian genetic algorithm and an empirical binding free energy function, *J. Comput. Chem.*, 1998, **19**, 1639–1662.
41 A. W. Schuettelkopf and D. M. F. van. Aalten, PRODRG-a tool for high-throughput crystallography of protein–ligand complexes, *Acta Crystallogr., Sect. D: Biol. Crystallogr.*, 2004, **D60**, 1355–1363.
42 M. J. Frisch, G. W. Trucks, H. B. Schlegel *et al.*, *Gaussian*, Inc., Pittsburgh PA, 2003.
43 E. Lindahl, B. Hess and D. von der Spoel, Gromacs 3.0: A package for molecular simulation and trajectory analysis, *J. Mol. Mod.*, 2001, **7**, 306–317.
44 W. F. van Gunsteren, S. R. Billeter, A. A. Eising, P. H. Hunenberger, P. Kruger, A. E. Mark, W. R. P. Scott, I. G. Tironi, Biomolecular Simulation: The GROMOS96 manual and user guide. Zurich, Switzerland: Hochschulverlag AG an der ETH Zürich. 1996.
45 B. Hess, H. Bekker, H. J. C. Berendsen and J. G. E. M. Fraaije, LINCS: A linear constraint solver for molecular simulations, *J. Comput. Chem.*, 1997, **18**, 1463–1472.
46 T. Darden, D. York and L. Pedersen, Particle mesh Ewald: An N-log(N) method for Ewald sums in large systems, *J. Chem. Phys.*, 1993, **98**, 10089–10092.
47 H. J. C. Berendsen, J. P. M. Postma, W. F. van Gunsteren, A. Dinola and J. R. Haak, Molecular dynamics with coupling to an external bath, *J. Chem. Phys.*, 1984, **81**, 3684–3690.

 This journal is © The Royal Society of Chemistry 2011